Meteor science

Compressive strength of a skirting Daytime Arietid – first science results from low-cost Raspberry Pi-based meteor stations

Denis Vida[1,2,3], *Michael J. Mazur*[1,2], *Damir Šegon*[4], *Patrik Kukić*[5], *and Aleksandar Merlak*[6]

We present the first detailed reduction of a double-station meteor recorded solely by a low-cost Raspberry Pi-based meteor system and demonstrate the quality of the data. The reduced event was a Daytime Arietid with an entry angle of only $\sim 1°$ and it lasted for 2.5 s. It had a sun-skirting orbit and it reached an equilibrium temperature of over 1000 K at perihelion. Due to the low entry angle the dynamic pressure on the meteor slowly increased and the compressive strength could be precisely measured. The meteoroid fragmented into a long trail at around 1.3 kPa, a very low compressive strength which indicates a highly porous meteoroid which had its volatiles completely removed due to a high level of thermal processing.

Received 2018 July 3

1 Introduction

Since 2015 there is an ongoing effort to develop a low-cost meteor system based on Raspberry Pi single-board computers which would replace the costly meteor observation systems used today (Zubović et al., 2015). Vida et al. (2016) demonstrated novel meteor and fireball detection algorithms which can run on such computers. Vida et al. (2018b) showed the first observational results, and the quality of astrometric and photometric calibrations, as well as the feasibility of using low-cost CMOS IP cameras for meteor observations. CMOS rolling shutter cameras with the Sony IMX225 sensors (1280×720 resolution, 25 FPS) have yielded a limiting magnitude for stars of +5.5 with a 4 mm $f/1.2$ lens ($64° \times 35°$ FOV) under both dark and light-polluted skies.

A permanent testbed Raspberry Pi Meteor Station (RMS) was installed in June 2017 near Elginfield, Ontario, Canada. In mid-June 2018 a second station was installed near Tavistock (both sites operated by the UWO Meteor Physics Group), the distance between stations is about 45 km. After initial testing, the first orbits using the systems were calculated.

The initial astrometric calibration is performed manually on several tens of stars on a single image, and then automatically refined every night using 1000s of stars recorded throughout the night, up to the precision of 1/3 px (following the procedure of Šegon (2009)). The photometric calibration is done manually – we found that the IMX225 sensors have $\gamma = 1.0$, thus a linear fit between the logarithm of the sum of the star intensity and the star magnitude can be performed, were the line has a slope of -2.5 (by definition), while only the photometric offset is fitted (i.e. the intercept of the line). The calibration procedure is described in detail in Vida et al. (2018b). The photometric offsets were 10.2 and 10.6 for Elginfield and Tavistock, respectfully.

Figure 1 – RMS camera at Tavistock

In this paper we present a detailed reduction of one dynamically and physically interesting event, demonstrate the quality of the data obtained, and present the science potential of the systems.

2 A skirting Daytime Arietid meteor

On 2018 June 15 at $07^h15^m44^s$ UTC (03^h15^m local time), the second night of double-station operation, both stations observed a 2.5 s long meteor which spanned a large portion of fields of view of both cameras. Figures 2 and 3 show co-added images of the meteor from both stations.

After estimating the trajectory on automated astrometry picks using the Borovička (1990) lines of sight method we noticed several peculiarities:

- the entry angle was very low, 0.5°
- the entry angle after the correction for Earth's gravity was around/below 0°
- there was virtually no deceleration
- the meteor climbed back up several tens of meters after the first half of the trajectory

[1]Department of Earth Sciences, University of Western Ontario, London, Ontario, N6A 5B7, Canada.
[2]Department of Physics and Astronomy, University of Western Ontario, London, Ontario, N6A 3K7, Canada.
[3]Email: dvida@uwo.ca
[4]Astronomical Society Istra Pula, Park Monte Zaro 2, HR-52100 Pula, Croatia
[5]XV Gymnasium, Jordanovac 8, HR-10000 Zagreb, Croatia
[6]Istrastream d.o.o., Hum, Croatia

IMO bibcode WGN-464-vida-arietid
NASA-ADS bibcode 2018JIMO...46..113V

Figure 2 – The image of the event from Elginfield (CA0001). The meteor was moving from right to left. The Polaris is in the upper centre, Cassiopeia is in the upper right.

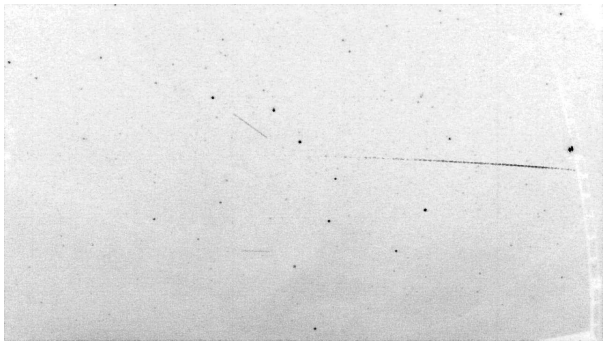

Figure 3 – The image of the event from Tavistock (CA0003). The meteor was moving from right to left. The big dipper dominates the centre of the image. An antenna mast is obstructing view of the beginning of the meteor, and thin clouds were present.

These were all indications of an Earth grazer, thus we decided to perform a more detailed manual reduction of the event using open source tools developed as a part of the RMS software package[a]. Figure 4 shows the manual reduction procedure.

Although Four-frame Temporal Pixel compression was used (Jenniskens et al., 2011), the RMS fireball detector detected the meteor in real time and stored its raw video frames which were showing that the meteor developed a long trail which influenced the positions of automated centroids. Figure 5 shows the mosaics of raw frame cut-outs from the Elginfield station. Due to the horizontal orientation of the meteor on the image and its slow on-chip angular velocity, the centroid correction for the rolling shutter effect was not needed. The effect of a rolling shutter on meteor centroids and the proposed correction will be elaborated in a future paper.

After a careful manual reduction where only the head of the meteor was centroided and the trail was excluded, the entry angle changed to $1.4° \pm 0.2°$, but the gravity-corrected entry angle was still $-0.4° \pm 0.2°$, making it a possible Earth grazer. Nevertheless, after the manual reduction the meteor did not climb up, but always descended down the atmosphere. Despite the ground track of almost 120 km (Figure 6) and the duration of 2.5 s, the meteor ended at 95.8 km, only 2 km below its beginning height. We believe that if the meteoroid was larger, it would have returned to interplanetary space, but it seems that the whole mass ablated away.

[a]Software is available on our GitHub page at: `https://github.com/CroatianMeteorNetwork/RMS`

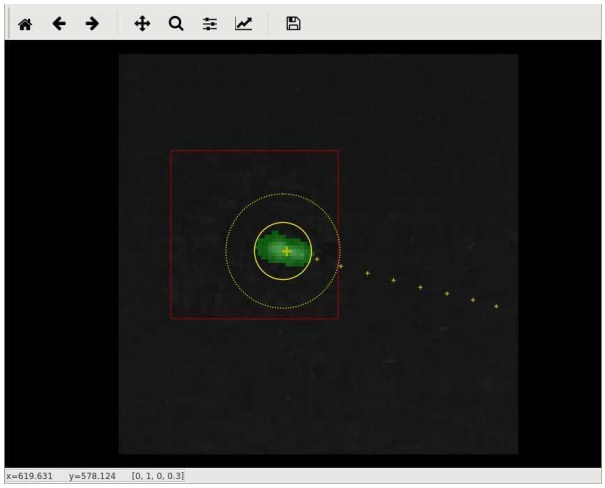

Figure 4 – Manual reduction procedure. The image is zoomed in around the meteor. The yellow circle is the centroiding annulus, the large yellow cross is the centroid on the current frame and small crosses are centroid on previous frames. The green transparent pixels are the pixels included in the photometry, and the red square is the raw frame cut-out.

The indicators of the quality of the reduction are the angular residuals of the trajectory fit shown in Figure 7. The standard deviation of the residuals from both stations is around 1 arc minute, which corresponds to the average precision of the astrometric fit (1/3 px). The scale of the image with the used cameras and lenses is around 3 arc minutes per pixel. The standard deviation of the spatial residuals from both sites was around 40 meters.

The initial velocity was estimated by performing a linear regression on time vs. length of the first 25% of the trajectory. The illustrate the deceleration of the meteor, we compute the lag, i.e. the difference in along-track position between the observed meteor and a hypothetical non-decelerating meteor. Figure 8 shows the observed lag from both stations. The meteor started to decelerate about 0.5 s after detection and stopped decelerating about 1 s after that. Note that the lag from Tavistock (CA0003) does not match the Elginfield lag well in the beginning as the meteor was passing behind a mast which made the determination of its position uncertain. Figure 9 shows the instantaneous velocities of the meteor – note that the velocity does not change much, it is nearly constant at $v = 42$ km s^{-1}.

The photometry was also performed manually. Every pixel that was a part of the meteor was "colored in" and the sum of the intensity of all marked pixels were taken. The comparison of absolute magnitudes (visual magnitudes normalized to 100 km) is shown in Figure 11. The error bars represent the photometric uncertainty. The two light curves deviate more around the peak brightness of the meteor due to a thin layer of clouds present at Tavistock (CA0003), which led to the underestimation of the brightness of the meteor. The

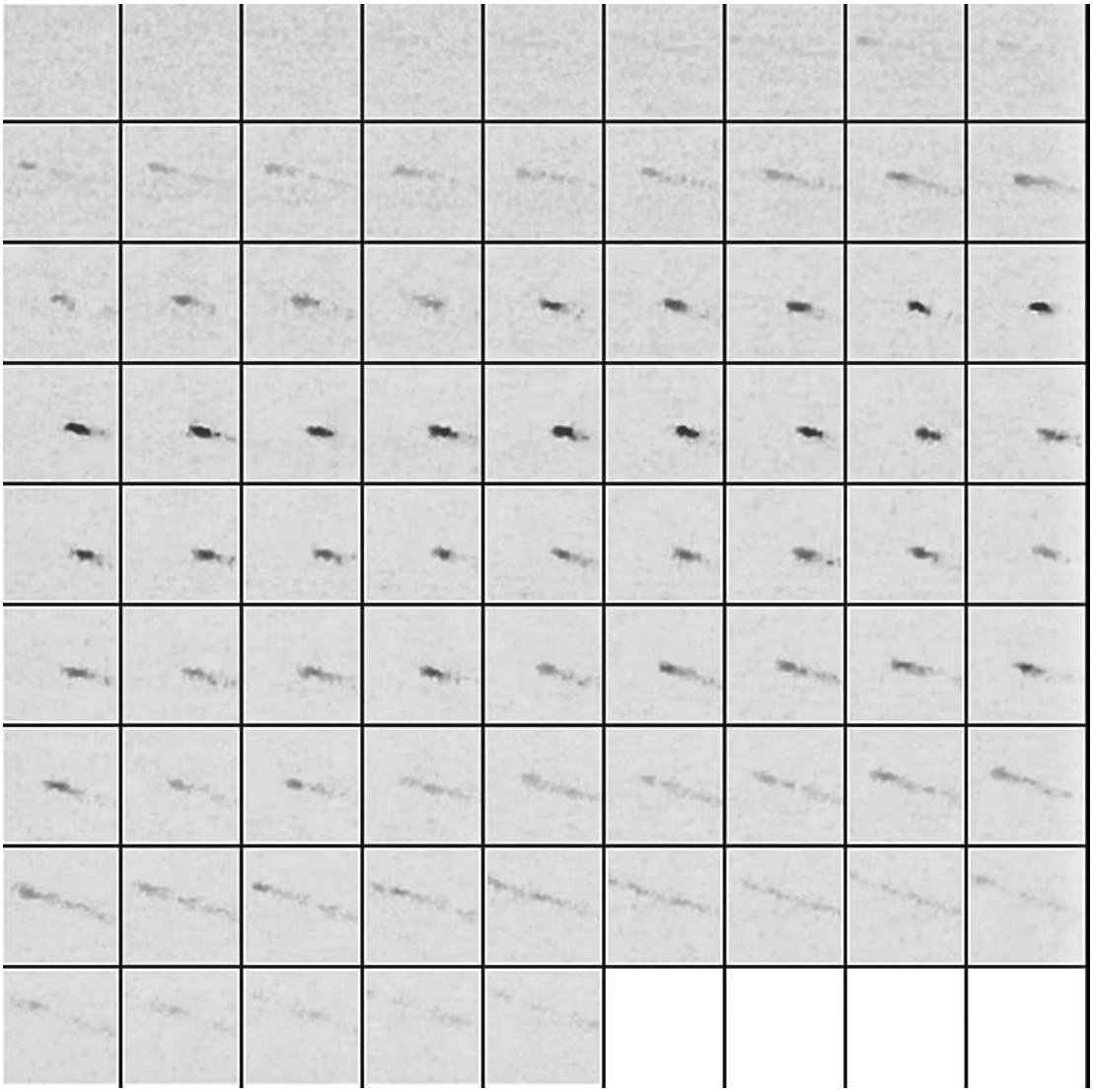

Figure 5 – Raw frame cut-outs from Elginfield. The event is showing a large trail.

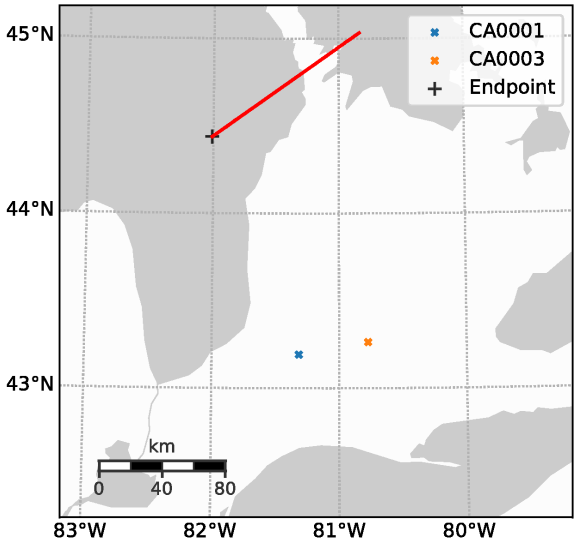

Figure 6 – Ground track of the event. CA0001 is the Elginfield station, and CA0003 is the Tavistock station. Lake Huron is in the upper left, Lake Earie at the bottom.

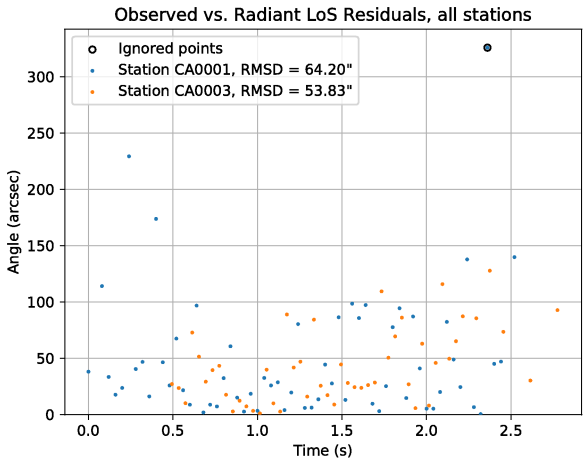

Figure 7 – Angular residuals of the trajectory fit. RMSD is root-mean-square deviation. Note that the deviation is higher at the beginning and the end as the meteor was fainter, thus the centroids were more uncertain due to a lower SNR.

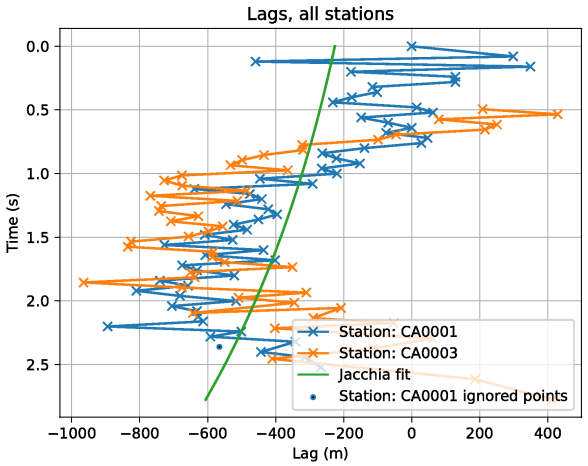

Figure 8 – The lag, i.e. the deceleration profile of the event. An operational fit of the Whipple & Jacchia (1957) exponential deceleration function was performed on the lag, but it does not represent the deceleration well.

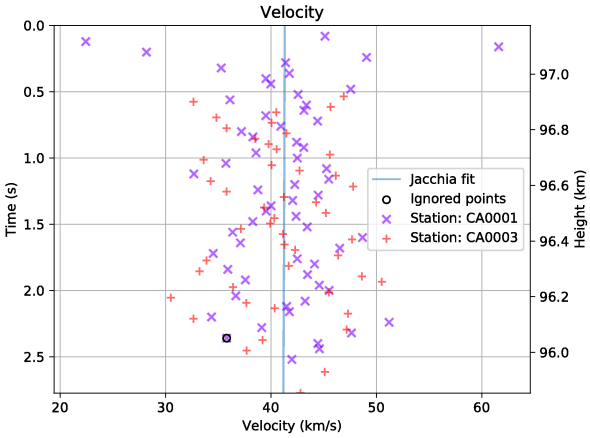

Figure 9 – Instantaneous velocities of the event.

photometric mass of the meteoroid was 0.2 g, assuming a dimensionless luminous efficiency of $\tau = 0.7\%$ and the power of a zero-magnitude meteor of $P_{0M} = 1210$ W (the value is taken for Sony HAD cameras from Weryk & Brown (2013)).

3 The orbit and physical properties of the meteoroid

The orbit of the meteoroid is interesting as well. It is shown in Figure 10 and details are given in Table 1. The uncertainties were estimated by adding Gaussian noise with the standard deviation estimated from the fit residuals (see Figure 7) and refitting the trajectory 100 times. The convergence angle was only 3°, but we are confident in the quality of the trajectory due to the well matching deceleration between both stations. The high uncertainty in declination is due to the limited geometry.

The meteor was a Daytime Arietid coming from the helion source – the shower association was determined

Table 1 – Orbital parameters of the meteoroid

Parameter	Value	Uncertainty
RA_g	48 °.83	±0 °.09
Dec_g	+24 °.01	±0 °.32
V_g	40.57 km s^{-1}	±0.26 km s^{-1}
$\lambda_\odot$	83 °.91	
a	1.96 AU	±0.07 AU
q	0.053 AU	±0.001 AU
e	0.973	±0.001
peri	22 °.58	±0 °.39
node	83 °.92	
i	25 °.53	±1 °.25

using the values from the IAU MDC database[b]. The perihelion distance was only $q = 0.052$ AU, and the eccentricity $e = 0.9734$, which classifies the orbit as a sun-skirter (Jones et al., 2018). The most recent perihelion was on May 13, only 33 days before it was observed. Even assuming a high Bond albedo of the particle of 0.5, the equilibrium temperature of the meteoroid at perihelion reaches over 1000 K, and due to its small size we can assume that is was heated throughout. At these temperatures for millimetre-sized meteoroids, all ices and volatiles sublimate within minutes (Crifo, 1995), leaving only refractory material behind. Furthermore, at the given perihelion of $\sim 11 R_\odot$ (solar radii) it is expected that all iron, magnetite and olivine sublimate too (Mann et al., 2004).

The meteoroid probably originated from comet 96P/Machholz (Abedin et al., 2017). Its significantly smaller semi-major axis indicates significant Poynting-Robertson (PR) evolution. As the period of the meteoroid is only 2.7 years, it had probably undergone multiple perihelion passages and is heavily thermally processed. Furthermore, we note that the estimated semi-major axis of 2 AU is more consistent with Daytime Arietid radar orbits (Brown et al., 2008) than with optical orbits (2.87 AU) (Jenniskens et al., 2018), a peculiarity which Abedin et al. (2017) too attribute to the PR drag that is acting on smaller meteoroids. On the other hand, the high eccentricity is unusual for PR evolved particles, as a more circular orbit would be expected. Nevertheless, PR drag is not as efficient on meteoroids with high eccentricities (Wyatt & Whipple, 1950).

3.0.1 Compressive strength

We use the dynamic pressure exerted on the meteor by the atmosphere at the moment of fragmentation as a proxy for the compressive strength of the meteoroid (Trigo-Rodriguez & Llorca, 2006; Borovička et al., 2007). Due to the low entry angle, the velocity and the height of the meteoroid do not change rapidly, thus the dynamic pressure on the meteoroid can be precisely estimated (Vida et al., 2018a). The dynamic pressure is simply computed as:

[b]IAU MDC database – Daytime Arietids: `http://pallas.astro.amu.edu.pl/~jopek/MDC2007/Roje/pojedynczy_obiekt.php?kodstrumienia=00171`

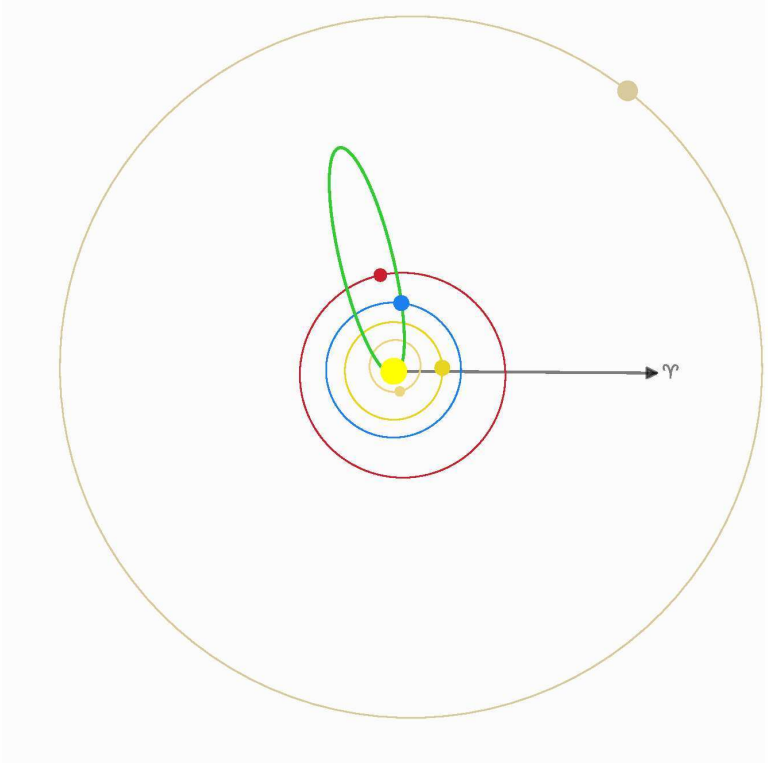

Figure 10 – The orbit of the event is shown in green. The sizes of orbits and planets are not to scale.

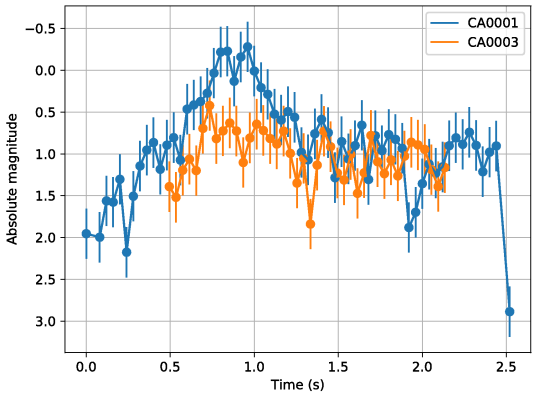

Figure 11 – Light curve of the event.

$$P_{dyn} = \Gamma v^2 \rho_{atm} \quad (1)$$

where Γ is the drag coefficient (assumed to be unity, as in Borovička et al. (2007)), v is the velocity of the meteor at the given point in time, and ρ_{atm} is the atmosphere mass density at the corresponding height. The atmosphere densities were taken from the NRLMSISE-00 atmosphere model (Picone et al., 2002).

At the brightest point on the trajectory, after which the meteor developed a long trail, the dynamic pressure was around 1.3 kPa. We believe that this value reflects the true compressive strength of the meteoroid due to the absence of a volatile matrix which would evaporate at temperatures > 1000 K (Campbell-Brown & Koschny, 2004). Due to such a low strength, the temperature of the meteoroid probably did not exceed the temperature needed to melt silicates, thus the removal of volatiles resulted in a very porous meteoroid which disintegrated after the dynamic pressure exceeded its compressive strength. The long trail might have been caused by thermal erosion (Borovička et al., 2007), but Vida et al. (2018) observed a similar low entry angle event with the Canadian Automated Meteor Observatory's high-resolution mirror tracking system and concluded that the observed distinct fragments separated due to the meteoroid being crushed.

4 Conclusion

We present the first detailed reduction of a double-station meteor using low-cost Raspberry Pi-based meteor stations. The astrometric precision of the cameras is approximately 1 arc minute and the photometric precision is close to 0.2 mag. The reduced meteor was a Daytime Arietid with a very low perihelion distance which had undergone extensive thermal processing at temperatures over 1000 K. As the meteor had a very low entry angle of $\sim 1°$, we were able to precisely measure the compressive strength of the meteoroid. The strength was only 1.3 kPa, an indication of a very weak object comparable to cinder. We believe the meteoroid was a highly porous object (all volatiles absent), and that it experienced a slow mechanical breakup in the atmosphere.

5 Acknowledgements

We thank Peter Gural for reviewing the manuscript of this paper.

6 Author Contributions

DV did the analysis and wrote the paper, MJM helped to install the hardware and reviewed the manuscript, DŠ provided comments and guidance, PK worked on investigating the influence of a rolling shutter on meteor centroids, and AM tested IP cameras and RMS software.

References

Abedin A., Wiegert P., Pokornỳ P., and Brown P. (2017). "The age and the probable parent body of the daytime arietid meteor shower". *Icarus*, **281**, 417–443.

Borovička J., Spurny P., and Koten P. (2007). "Atmospheric deceleration and light curves of Draconid meteors and implications for the structure of cometary dust". *Astronomy & Astrophysics*, **473:2**, 661–672.

Borovička J. (1990). "The comparison of two methods of determining meteor trajectories from photographs". *Bulletin of the Astronomical Institutes of Czechoslovakia*, **41**, 391–396.

Brown P., Weryk R., Wong D., and Jones J. (2008). "A meteoroid stream survey using the Canadian Meteor Orbit Radar: I. Methodology and radiant catalogue". *Icarus*, **195:1**, 317–339.

Campbell-Brown M. and Koschny D. (2004). "Model of the ablation of faint meteors". *Astronomy & Astrophysics*, **418:2**, 751–758.

Crifo J. (1995). "A general physicochemical model of the inner coma of active comets. 1: Implications of spatially distributed gas and dust production". *The Astrophysical Journal*, **445**, 470–488.

Jenniskens P., Baggaley J., Crumpton I., Aldous P., Pokorny P., Janches D., Gural P. S., Samuels D., Albers J., Howell A., et al. (2018). "A survey of southern hemisphere meteor showers". *Planetary and Space Science*.

Jenniskens P., Gural P., Dynneson L., Grigsby B., Newman K., Borden M., Koop M., and Holman D. (2011). "CAMS: Cameras for Allsky Meteor Surveillance to establish minor meteor showers". *Icarus*, **216:1**, 40–61.

Jones G. H., Knight M. M., Battams K., Boice D. C., Brown J., Giordano S., Raymond J., Snodgrass C., Steckloff J. K., Weissman P., et al. (2018). "The science of sungrazers, sunskirters, and other near-sun comets". *Space Science Reviews*, **214:1**, 20.

Mann I., Kimura H., Biesecker D. A., Tsurutani B. T., Grün E., McKibben R. B., Liou J.-C., MacQueen R. M., Mukai T., Guhathakurta M., et al. (2004). "Dust near the Sun". *Space Science Reviews*, **110:3-4**, 269–305.

Picone J., Hedin A., Drob D. P., and Aikin A. (2002). "NRLMSISE-00 empirical model of the atmosphere: Statistical comparisons and scientific issues". *Journal of Geophysical Research: Space Physics*, **107:A12**, SIA–15.

Trigo-Rodriguez J. M. and Llorca J. (2006). "The strength of cometary meteoroids: Clues to the structure and evolution of comets". *Monthly Notices of the Royal Astronomical Society*, **372:2**, 655–660.

Vida D., Brown P., Campbell-Brown M., and Huggins S. (2018a). "Canadian Automated Meteor Observatory: Cometary meteoroid strengths derived from a highly fragmenting event observed on July 21, 2017". In *Proceedings of the International Meteor Conference (IMC2017), Petnica, Serbia*.

Vida D., Mazur M., Šegon D., Zubovič D., Kukič P., Parag F., and Macan A. (2018b). "First results of a Raspberry Pi based meteor camera system". *WGN, Journal of the International Meteor Organization*, **46:2**, 71–78.

Vida D., Zubović D., Šegon D., Gural P., and Cupec R. (2016). "Open-source meteor detection software for low-cost single-board computers". In *Proceedings of the International Meteor Conference (IMC2016), Egmond, The Netherlands*. pages 2–5.

Šegon D. (2009). "How many stars are needed for a good camera calibration?". *WGN, Journal of the International Meteor Organization*, **37:3**, 80–83.

Weryk R. J. and Brown P. G. (2013). "Simultaneous radar and video meteors – II: Photometry and ionisation". *Planetary and Space Science*, **81**, 32–47.

Whipple F. L. and Jacchia L. G. (1957). "The orbits of 308 meteors photographed with super-Schmidt cameras". *The Astronomical Journal*, **62**, 37.

Wyatt S. P. and Whipple F. L. (1950). "The Poynting-Robertson effect on meteor orbits". *The Astrophysical Journal*, **111**, 134–141.

Zubović D., Vida D., Gural P., and Šegon D. (2015). "Advances in the development of a low-cost video meteor station". In *Proceedings of the International Meteor Conference, Mistelbach, Austria*. pages 27–30.

Handling Editor: Javor Kac

This paper has been typeset from a LaTeX file prepared by the authors.